

W production at large transverse momentum at the Large Hadron Collider

Richard J. Gonsalves,^a Nikolaos Kidonakis,^b and Agustín Sabio Vera^c

^a *Department of Physics, University at Buffalo, The State University of New York
Buffalo, NY 14260-1500*

^b *Kennesaw State University, Physics #1202
1000 Chastain Rd., Kennesaw, GA 30144-5591, USA*

^c *II. Institut für Theoretische Physik, Universität Hamburg
Luruper Chaussee 149, 22761 Hamburg, Germany*

Abstract

We study the production of W bosons at large transverse momentum in pp collisions at the Large Hadron Collider (LHC). We calculate the complete next-to-leading order (NLO) corrections to the differential cross section. We find that the NLO corrections provide a large increase to the cross section but, surprisingly, do not reduce the scale dependence relative to leading order (LO). We also calculate next-to-next-to-leading-order (NNLO) soft-gluon corrections and find that, although they are small, they significantly reduce the scale dependence thus providing a more stable theoretical prediction.

1 Introduction

The study of W -boson production in hadron colliders is important in testing the Standard Model [1] and in estimating backgrounds to Higgs production and new physics [2]. Precise theoretical predictions for W production at the Large Hadron Collider (LHC) are needed to exploit fully the large number of such events that are anticipated when the LHC begins operation in 2007. Accurate predictions for this process, which has a particularly clean experimental signature when the W decays to leptons, are needed to reduce the systematic uncertainties in precision measurements, e.g., of the W mass and decay width. Due to the large number of events expected, this process can also be used to determine the parton-parton luminosity [3]. Furthermore, accurate calculations for W production at large transverse momentum, Q_T , are required to distinguish the Standard Model prediction from signals of possible new physics, such as new gauge bosons and extra dimensions [4], which may be expected to enhance the Q_T distribution at large Q_T .

Calculations of the next-to-leading order (NLO) cross section for W production at large transverse momentum at the Fermilab Tevatron collider were presented in Refs. [5, 6]. These predictions have been tested experimentally by the CDF and DØ collaborations [7], and found to be consistent with the data at large Q_T . The NLO corrections contribute to enhance the differential distributions in Q_T of the W boson and they reduce the factorization and renormalization scale dependence of the cross section. A recent study [8] included soft-gluon corrections through next-to-next-to-leading order (NNLO), which provide additional enhancements and a further reduction of the scale dependence.

At leading order (LO) in the Quantum Chromodynamic (QCD) coupling α_s , a W -boson can be produced at large Q_T by recoiling against a single parton which decays into a jet of hadrons. The NLO corrections to this cross section involve one-loop parton processes with a virtual gluon, and real radiative processes with two partons in the final state. The virtual corrections involve ultraviolet divergences which renormalize α_s and cause it to depend on a renormalization energy scale which we will take to be $\sim Q_T$. Both real and virtual corrections have soft and collinear divergences which arise from the masslessness of the gluons and our approximation of zero masses for the quarks. The soft divergences cancel between real and virtual processes. The net collinear singularities are factorized in a process-independent manner and absorbed into factorization-scale-dependent parton distribution functions. Complete analytic expressions for the inclusive NLO cross sections in terms of the partonic Mandelstam variables were presented in Refs. [5, 6], and form the basis for the NLO results in this work.

The calculation of hard-scattering cross sections near partonic threshold, such as W -boson production at large transverse momentum, involves corrections from the emission of soft gluons from the partons in the process. At each order in perturbation theory one encounters large logarithms that arise from the cancellations between real emission and virtual processes, due to the limited phase space available for real gluon emission near partonic threshold. These threshold corrections formally exponentiate as a result of the factorization properties [9] of the cross section. Expansions of the resummed cross section can be derived in principle to any higher order. A unified approach to the calculation of NNLO soft-gluon corrections for hard-scattering processes was recently presented in Ref. [10]. Analytic expressions for W production are given in Ref. [8].

We note that there has also been work on resummation of Sudakov logarithms at small transverse momentum for electroweak boson production in hadron colliders [11, 12, 13, 14] as well as on joint resummation of Q_T and threshold logarithms [15]. The results presented in this paper for large $Q_T \geq 20$ GeV are not sensitive to this resummation.

In this paper we calculate the complete NLO corrections as well as the NNLO soft-gluon corrections for W -boson production at large transverse momentum at the LHC. We study the size of the corrections and their significance in stabilizing the cross section versus changes in the factorization and renormalization scales.

2 Kinematics and Partonic Cross Sections

For the production of a W boson, with momentum Q , in collisions of two hadrons h_A and h_B with momenta P_A and P_B

$$h_A(P_A) + h_B(P_B) \longrightarrow W(Q) + X, \quad (2.1)$$

where X denotes all additional particles in the final state, we can write the factorized single-particle-inclusive cross section as

$$E_Q \frac{d\sigma_{h_A h_B \rightarrow W(Q)+X}}{d^3Q} = \sum_{f_a, f_b} \int dx_a dx_b \phi_{f_a/h_A}(x_a, \mu_F^2) \phi_{f_b/h_B}(x_b, \mu_F^2) \times E_Q \frac{d\hat{\sigma}_{f_a f_b \rightarrow W(Q)+X}}{d^3Q}(s, t, u, Q^2, \mu_F, \mu_R, \alpha_s(\mu_R^2)) \quad (2.2)$$

where $E_Q = Q^0$, the parton distribution $\phi_{f/h}$ is the probability density in the momentum fraction x for finding parton f with momentum $p = xP$ in hadron h , and $\hat{\sigma}$ is the perturbative parton-level cross section. The initial-state collinear singularities are factorized into the parton distributions at factorization scale μ_F , while μ_R is the renormalization scale.

At the parton level, the lowest-order subprocesses for the production of a W boson and a parton involve quarks q , anti-quarks \bar{q} and gluons g :

$$\begin{aligned} q(p_a) + g(p_b) &\longrightarrow W(Q) + q(p_c), \\ q(p_a) + \bar{q}(p_b) &\longrightarrow W(Q) + g(p_c). \end{aligned} \quad (2.3)$$

The partonic kinematical invariants in the process are $s = (p_a + p_b)^2$, $t = (p_a - Q)^2$, $u = (p_b - Q)^2$, and $s_2 = s + t + u - Q^2 = (p_a + p_b - Q)^2$. Here s_2 is the invariant mass of the system recoiling against the electroweak boson at the parton level and parameterizes the inelasticity of the parton scattering, taking the value $s_2 = 0$ for one-parton production.

Schematically, the parton level cross sections at NLO have the form

$$E_Q \frac{d\hat{\sigma}_{f_a f_b \rightarrow W(Q)+X}}{d^3Q} = \delta(s_2) \alpha_s(\mu_R^2) \left[A(s, t, u) + \alpha_s(\mu_R^2) B(s, t, u, \mu_R) \right] + \alpha_s^2(\mu_R^2) C(s, t, u, s_2, \mu_F). \quad (2.4)$$

The coefficient functions A , B and C depend on the parton flavors $f_a f_b$ and on electroweak parameters (which are suppressed), in addition to the kinematic variables s, t, u, s_2 , and scales

μ_R, μ_F shown explicitly. The coefficient $A(s, t, u)$ arises from the LO processes in Eq. (2.3). The functions B and C result from a perturbative QCD calculation of the virtual and real corrections, respectively, to the processes (2.3). The NLO calculation is done using dimensional regularization and modified minimal subtraction ($\overline{\text{MS}}$) to deal with ultraviolet, soft, and collinear divergences. The function $B(s, t, u, \mu_R)$ is the finite (after renormalization) sum of virtual corrections and of singular terms $\sim \delta(s_2)$ in the real radiative corrections. The function $C(s, t, u, s_2, \mu_F)$ is the finite (after factorization) contribution from real emission processes away from the edge $s_2 = 0$ of phase space. Analytic expressions for these functions from Ref. [6] were used to compute the numerical NLO results in this paper.

In general, the partonic cross section $\hat{\sigma}$ includes distributions with respect to s_2 at n -th order in the QCD coupling α_s of the type

$$\left[\frac{\ln^m(s_2/Q_T^2)}{s_2} \right]_+, \quad m \leq 2n - 1, \quad (2.5)$$

defined by their integral with any smooth function f by

$$\int_0^{s_{2max}} ds_2 f(s_2) \left[\frac{\ln^m(s_2/Q_T^2)}{s_2} \right]_+ \equiv \int_0^{s_{2max}} ds_2 \frac{\ln^m(s_2/Q_T^2)}{s_2} [f(s_2) - f(0)] + \frac{1}{m+1} \ln^{m+1} \left(\frac{s_{2max}}{Q_T^2} \right) f(0). \quad (2.6)$$

These “plus” distributions are the remnants of cancellations between real and virtual contributions to the cross section. Below we will make use of the terminology that at n -th order in α_s the leading logarithms (LL) are those with $m = 2n - 1$ in Eq. (2.5), the next-to-leading logarithms (NLL) are those with $m = 2n - 2$, the next-to-next-to-leading logarithms (NNLL) are those with $m = 2n - 3$, and the next-to-next-to-next-to-leading logarithms (NNNLL) are those with $m = 2n - 4$. Below the term “NNLO-NNNLL” means that the soft-gluon contributions through NNNLL to the NNLO corrections have been included and added to the complete NLO result (for details see Ref. [8]).

3 Numerical results

We now apply our results to W production at large transverse momentum at the LHC. Throughout we use the MRST2002 parton densities [16]. The QCD coupling $\alpha_s(\mu_R^2/\Lambda^2)$ is computed using the appropriate value of the 4-flavor QCD scale parameter Λ_4 required by the LO, NLO, and NNLO parton densities, and assuming five flavors of quarks (u,d,s,c,b). The coupling is evolved using the massless LO, NLO and NNLO β -function as appropriate, and using the standard [1] effective-flavor scheme to cross heavy-quark thresholds. The electroweak coupling $\alpha(M_Z^2)$ is evaluated at the mass of the Z boson, and standard values [1] are used for the various electroweak parameters.

In all of the numerical results we present the sum of cross sections for W^- and W^+ production. W bosons at the LHC will be detected primarily through their leptonic decay products e.g., $W^- \rightarrow \ell \bar{\nu}_\ell$. Our cross sections should therefore be multiplied by the appropriate branching

$pp \rightarrow W \quad \sqrt{S}=14 \text{ TeV} \quad \mu=Q_T$

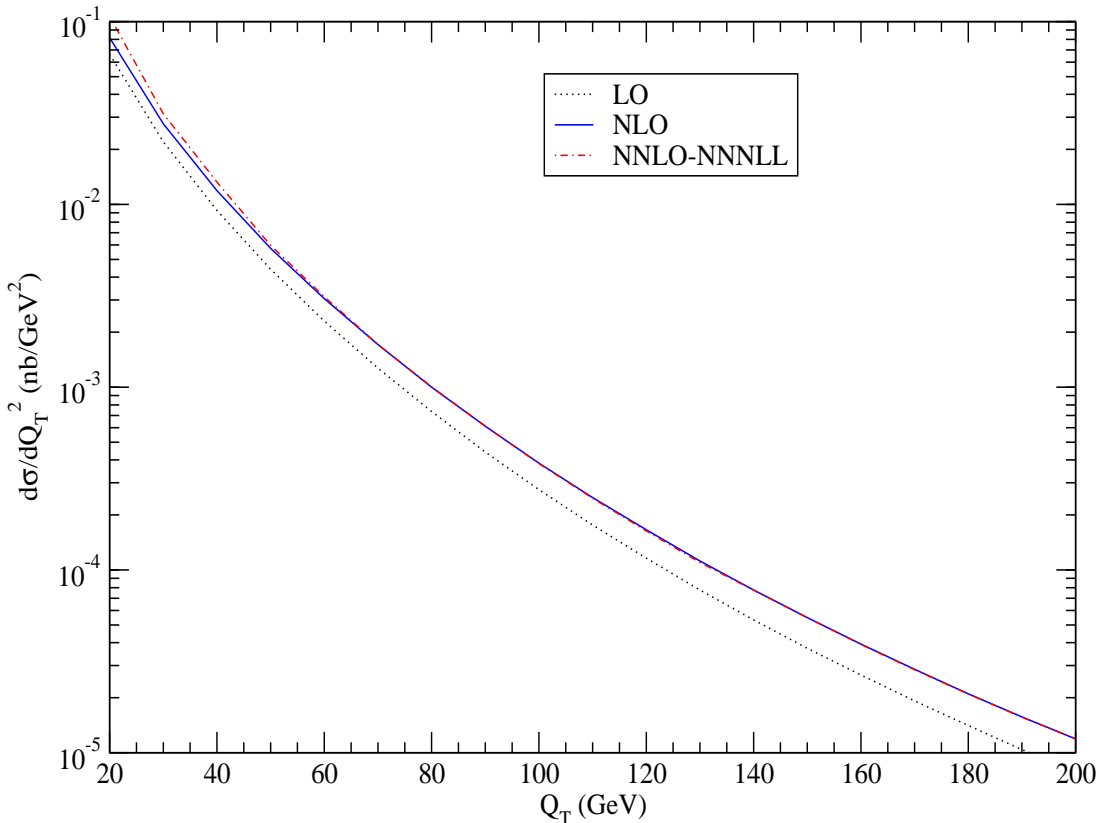


Figure 1: The differential cross section, $d\sigma/dQ_T^2$, for W production in pp collisions at the LHC with $\sqrt{S} = 14$ TeV and $\mu = \mu_F = \mu_R = Q_T$. Shown are the LO, NLO, and NNLO-NNLL results.

ratios (~ 0.11 for each lepton species). Our cross sections are integrated over the full phase space of the W and final state partons. Detailed comparisons with experiment will require realistic cuts on lepton and jet momenta. These modifications will affect the overall normalization of the cross sections, but they should not affect the main results of this paper concerning the convergence and reliability of perturbative corrections.

In Fig. 1 we plot the transverse momentum distribution, $d\sigma/dQ_T^2$, for W production at the LHC with $\sqrt{S} = 14$ TeV. Here we set $\mu_F = \mu_R = Q_T$ and denote this common scale by μ . We plot LO, NLO, and NNLO-NNLL results. In the LO result we use LO parton densities, in the NLO result we use NLO parton densities, and in the NNLO-NNLL result we use NNLO parton densities. We see that the NLO corrections provide a significant enhancement of the LO Q_T distribution. The NNLO-NNLL corrections provide a further rather small enhancement of the Q_T distribution, which is hardly visible in the plot. Part of the reason for the small difference between the NLO and the NNLO-NNLL curves is that the NNLO parton densities reduce the cross section. As we will see below, the NNLO-NNLL corrections can be much

$$pp \rightarrow W \quad \sqrt{S} = 14 \text{ TeV} \quad \mu = Q_T$$

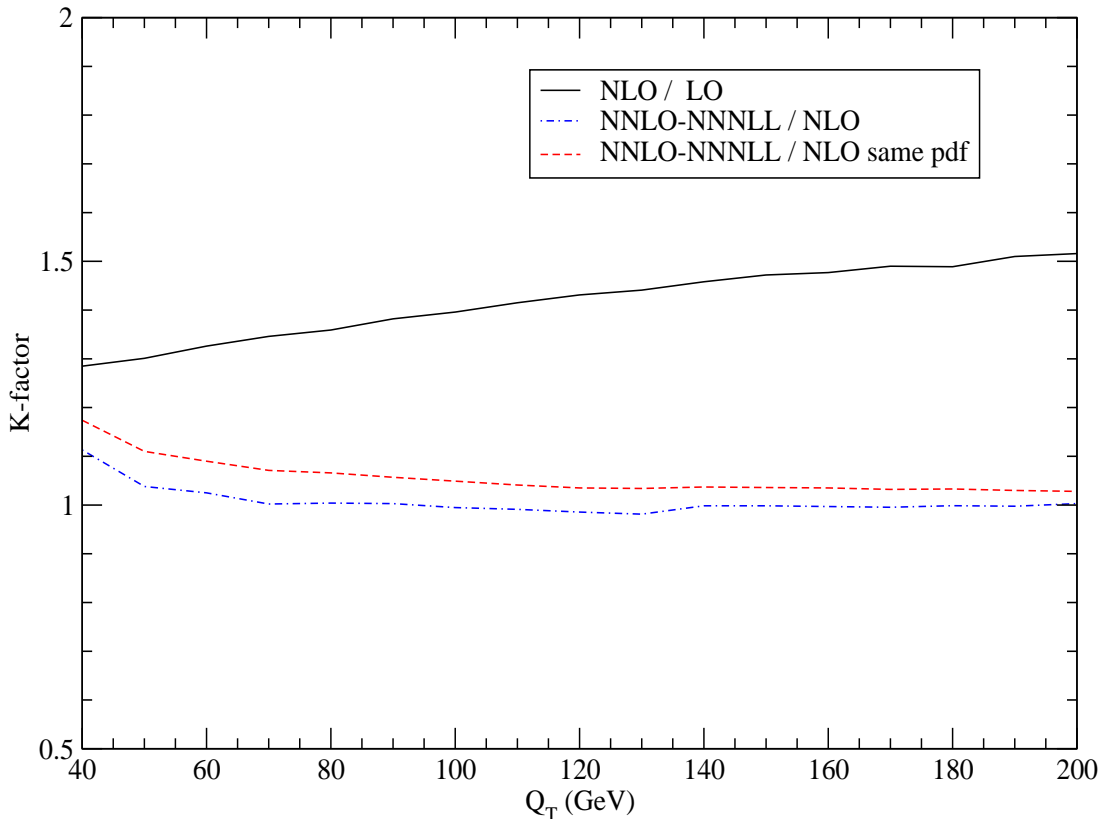


Figure 2: The K -factors for the differential cross section, $d\sigma/dQ_T^2$, for W production in pp collisions at the LHC with $\sqrt{S} = 14$ TeV and $\mu = \mu_F = \mu_R = Q_T$. Shown are the K - factors for NLO/LO and NNLO-NNLL/NLO. The latter is shown with the same or different parton distribution functions (pdf) for the NLO and NNLO results.

bigger for other choices of factorization and renormalization scales. We also note that the NNLO-NNLL result is practically the same as at NNLO-NNLL (i.e. if we had kept one level less of logarithms), and that while the LL, NLL, and NNLL terms are complete, the NNLL terms are not complete but include the dominant contributions (see [8] for details).

In Fig. 2 we plot the K -factors, i.e. the ratios of cross sections at various orders and accuracies to the LO cross section, all with $\mu_F = \mu_R = Q_T$, in the high- Q_T region. We see that the NLO/LO ratio is rather large; the NLO corrections increase the LO result by about 30% to 50% in the Q_T range shown. In contrast, the NNLO-NNLL/NLO ratio for this choice of scale is rather small. Part of the reason for this is that the NNLO parton densities are significantly smaller than the NLO parton densities. To make this point more clearly we also show a curve for the NNLO-NNLL/NLO K -factor where both the NNLO-NNLL and the NLO cross sections are calculated using the same NNLO parton densities. The ratio is then significantly bigger. We can also see that the NNLO-NNLL/NLO K -factors are nearly constant over the Q_T range

$pp \rightarrow W \quad \sqrt{S}=14 \text{ TeV} \quad Q_T=50 \text{ GeV}$

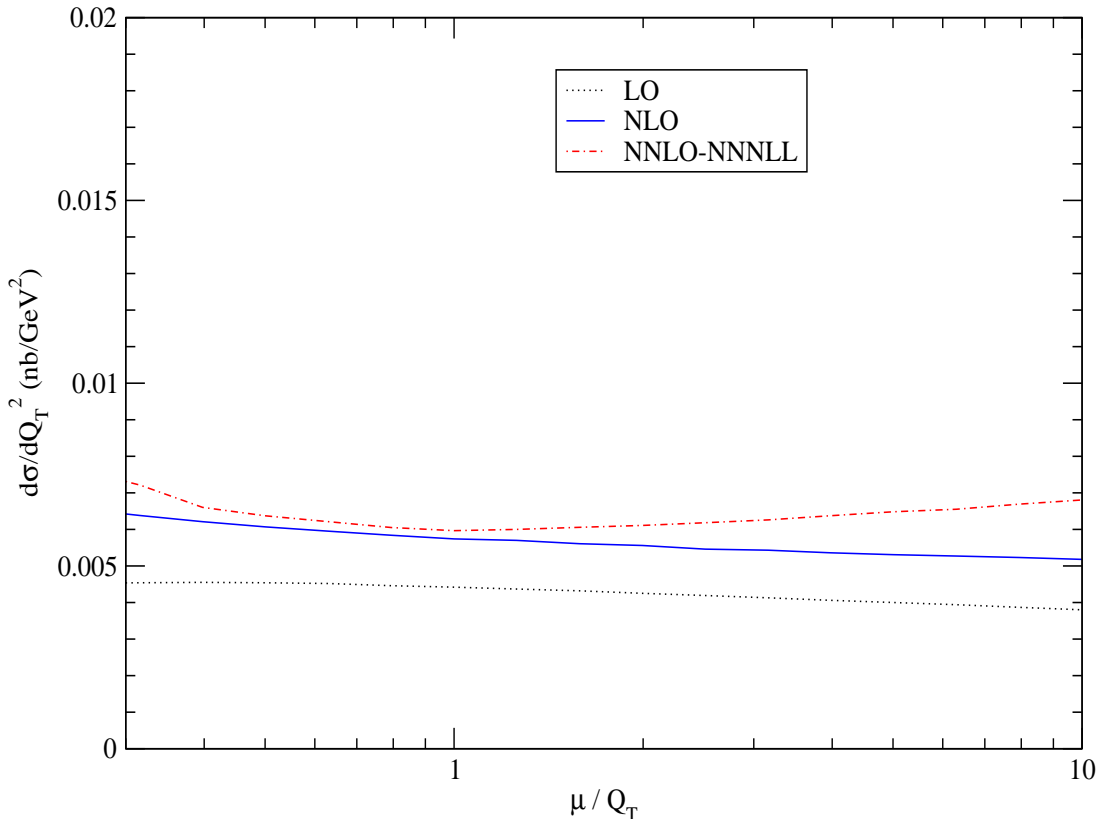


Figure 3: The differential cross section, $d\sigma/dQ_T^2$, for W production in pp collisions at the LHC with $\sqrt{S} = 14$ TeV, $Q_T = 50$ GeV, and $\mu = \mu_F = \mu_R$. Shown are the LO, NLO, and NNLO-NNLL results.

shown even though the differential cross sections themselves span three orders of magnitude in this range.

In Figs. 3, 4, and 5 we plot the scale dependence of the differential cross section for $Q_T = 50$, 80, and 150 GeV, respectively. We set $\mu_F = \mu_R$ and denote this common scale by μ . We plot the differential cross section versus μ/Q_T over two orders of magnitude. We note that the scale dependence of the cross section is not reduced when the NLO corrections are included, but we have an improvement when the NNLO-NNLL corrections are added. The NNLO-NNLL result approaches the scale independence expected of a truly physical cross section.

It is interesting, and perhaps a little surprising, that the scale dependence of the LO results in Figs. 3, 4, 5 is less pronounced than that of the NLO results. One might expect that the scale dependence should decrease with each successive order of perturbation theory. This is indeed what is observed at Tevatron energies [6, 8], where the LO cross section increases monotonically with decreasing scale and has positive curvature. The LO curves in Figs. 3, 4, 5 have little curvature, and at $Q_T = 80$ GeV the curve actually turns over at small μ/Q_T . In Fig. 6 we

$pp \rightarrow W \quad S^{1/2} = 14 \text{ TeV} \quad Q_T = 80 \text{ GeV}$

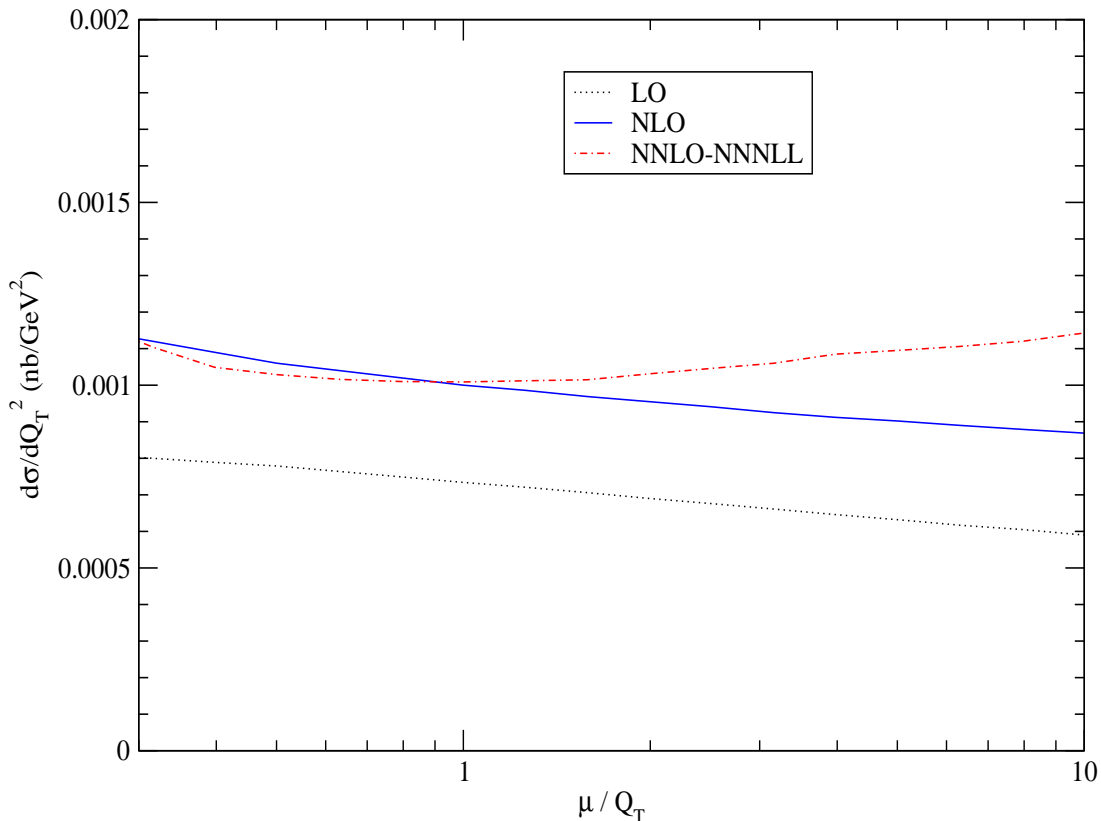


Figure 4: The differential cross section, $d\sigma/dQ_T^2$, for W production in pp collisions at the LHC with $\sqrt{S} = 14$ TeV, $Q_T = 80$ GeV, and $\mu = \mu_F = \mu_R$. Shown are the LO, NLO, and NNLO-NNLL results.

plot the LO scale dependence separately for μ_F and μ_R with the other held fixed. The cross section increases with positive curvature as the renormalization scale μ_R is decreased: this is the expected behavior at LO due to asymptotic freedom. The μ_F dependence however has negative curvature and the cross section increases with scale. This behavior is due to the fact that the cross section is dominated by the gluon-initiated process $qg \rightarrow Wq$. The gluon density in the proton increases rapidly with scale at fixed x smaller than ~ 0.01 . At LHC energies, the μ_R and μ_F dependencies cancel one another approximately, while the scale dependence of the LO cross section at Tevatron energies is dominated by the μ_R dependence of α_s .

In Fig. 7 we plot the differential cross section $d\sigma/dQ_T^2$ at high Q_T with $\sqrt{S} = 14$ TeV for two values of scale, $Q_T/2$ and $2Q_T$, often used to display the uncertainty due to scale variation. We note that while the variation of the LO cross section is significant and the variation at NLO is similar to LO, at NNLO-NNLL it is very small. In fact the two NNLO-NNLL curves lie very close to or on top of each other. These results are consistent with Figs. 3, 4, 5.

$pp \rightarrow W \quad \sqrt{S}=14 \text{ TeV} \quad Q_T=150 \text{ GeV}$

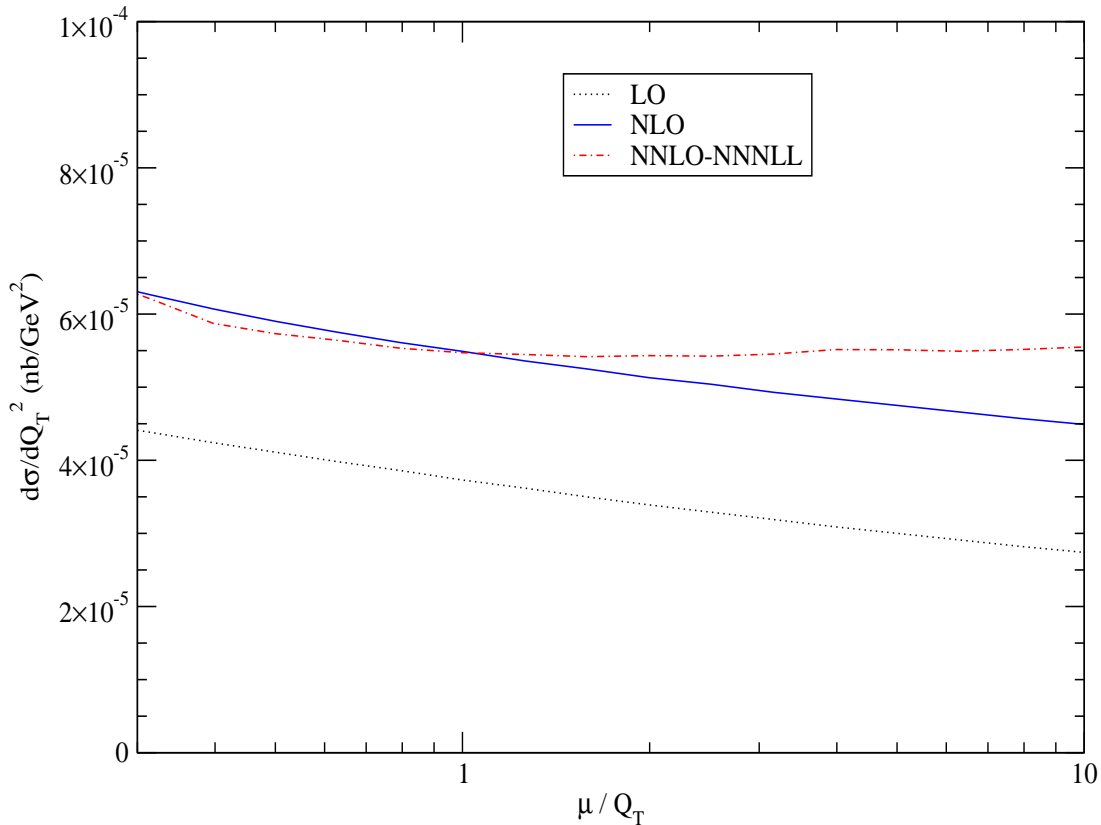


Figure 5: The differential cross section, $d\sigma/dQ_T^2$, for W production in pp collisions at the LHC with $\sqrt{S} = 14$ TeV, $Q_T = 150$ GeV, and $\mu = \mu_F = \mu_R$. Shown are the LO, NLO, and NNLO-NNLL results.

4 Conclusions

We have presented the full NLO and the NNLO soft-gluon corrections for W production at large transverse momentum in pp collisions at the LHC. We have shown that the NLO corrections are large but do not diminish the scale dependence of the cross section relative to LO. The NNLO-NNLL corrections are very small for $\mu = Q_T$ but they significantly decrease the factorization and renormalization scale dependence of the transverse momentum distributions. These precise and reliable perturbative QCD predictions for inclusive W production will facilitate precision tests of the Standard Model, measurements of parton densities, and searches for new physics at the LHC.

$pp \rightarrow W$ $\sqrt{S}=14$ TeV $Q_T=80$ GeV

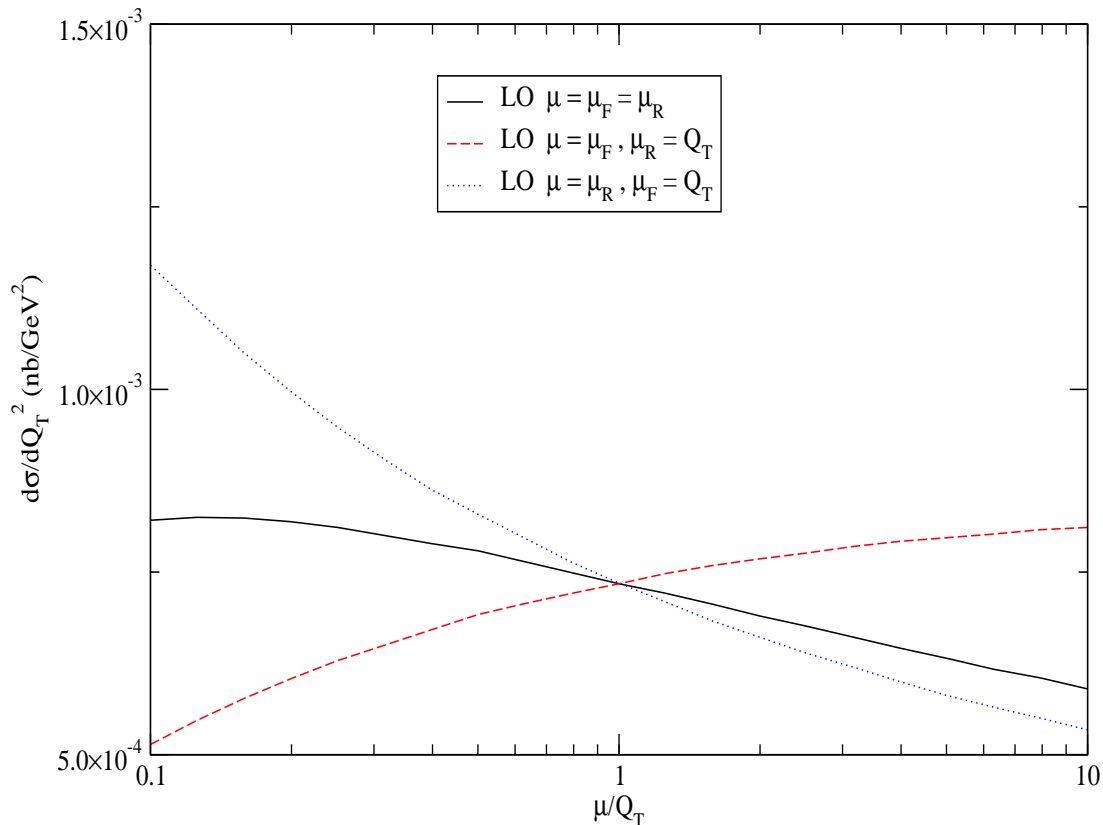


Figure 6: The differential cross section, $d\sigma/dQ_T^2$, for W production in pp collisions at the LHC with $\sqrt{S} = 14$ TeV, $Q_T = 80$ GeV. Shown are the LO results with $\mu_F = \mu_R$, and with μ_F and μ_R varied separately.

References

- [1] Particle Data Group, S. Eidelman *et al.*, Phys. Lett. B **592**, 1 (2004) summarizes the current status of the Standard Model.
- [2] See e.g., the summary reports of the Les Houches 2003 Workshop: Physics at TeV Colliders, M. Dobbs *et al.*, arXiv:hep-ph/0403100; K.A. Assamagan *et al.*, arXiv:hep-ph/0406152; B.C. Allanach *et al.*, arXiv:hep-ph/0402295.
- [3] M. Dittmar, F. Pauss, and D. Zurcher, Phys. Rev. D **56**, 7284 (1997); A.D. Martin, R.G. Roberts, W.J. Stirling, and R.S. Thorne, Eur. Phys. J. C **14**, 133 (2000).
- [4] Ref. [1] has reviews with extensive references on W' searches and extra dimensions. See also B.C. Allanach *et al.* in [2], J. Hewett and M. Spiropulu, Ann. Rev. Nucl. Part. Sci. **52**, 397 (2002).

pp --> W $S^{1/2}=14$ TeV $\mu=Q_T/2, 2Q_T$

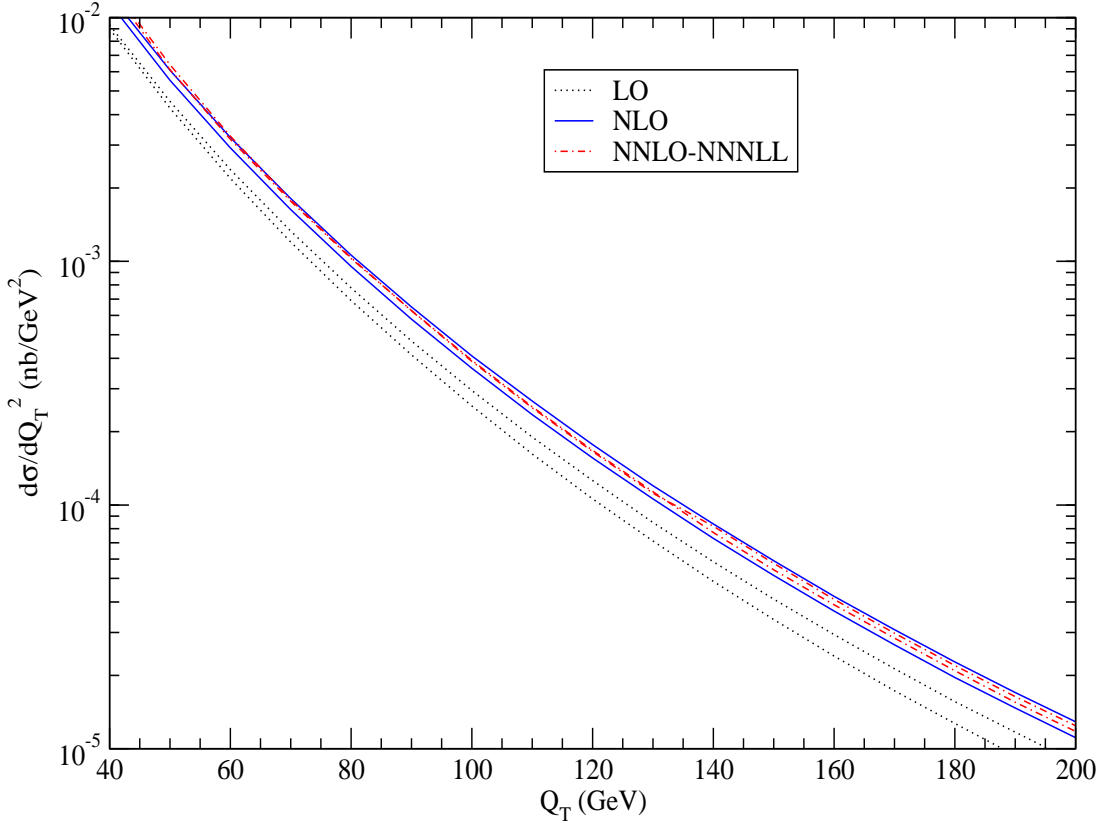


Figure 7: The differential cross section, $d\sigma/dQ_T^2$, for W production in pp collisions at the LHC with $\sqrt{S} = 14$ TeV and $\mu = \mu_F = \mu_R = Q_T/2$ or $2Q_T$. Shown are the LO, NLO, and NNLO-NNLL results. The upper lines are with $\mu = Q_T/2$, the lower lines with $\mu = 2Q_T$.

- [5] P.B. Arnold and M.H. Reno, Nucl. Phys. B **319**, 37 (1989); (E) B **330**, 284 (1990).
- [6] R.J. Gonsalves, J. Pawlowski, and C.-F. Wai, Phys. Rev. D **40**, 2245 (1989); Phys. Lett. B **252**, 663 (1990).
- [7] F. Abe *et al.* [CDF Collaboration], Phys. Rev. Lett. **66**, 2951 (1991); B. Abbott *et al.* [DØ Collaboration], Phys. Rev. Lett. **80**, 5498 (1998); Phys. Lett. B **513**, 292 (2001).
- [8] N. Kidonakis and A. Sabio Vera, JHEP **02**, 027 (2004).
- [9] N. Kidonakis and G. Sterman, Phys. Lett. B **387**, 867 (1996); Nucl. Phys. B **505**, 321 (1997); E. Laenen, G. Oderda, and G. Sterman, Phys. Lett. B **438**, 173 (1998); N. Kidonakis, Int. J. Mod. Phys. A **15**, 1245 (2000); N. Kidonakis and V. Del Duca, Phys. Lett. B **480**, 87 (2000).
- [10] N. Kidonakis, Int. J. Mod. Phys. A **19**, 1793 (2004); Mod. Phys. Lett. A **19**, 405 (2004).

- [11] R.K. Ellis, D.A. Ross, and S. Veseli, Nucl. Phys. B **503**, 309 (1997); R.K. Ellis and S. Veseli, Nucl. Phys. B **511**, 649 (1998).
- [12] C. Balazs and C.-P. Yuan, Phys. Rev. D **56**, 5558 (1997).
- [13] A. Kulesza and W.J. Stirling, Nucl. Phys. B **555**, 279 (1999); Eur. Phys. J. C **20**, 349 (2001).
- [14] P.M. Nadolsky and C.-P. Yuan, Nucl. Phys. B **666**, 3 (2003).
- [15] A. Kulesza, G. Sterman, and W. Vogelsang, Phys. Rev. D **66**, 014011 (2002).
- [16] A.D. Martin, R.G. Roberts, W.J. Stirling, and R.S. Thorne, Eur. Phys. J. C **28**, 455 (2003).